



*Dedicated to the memory of
Academician Bogdan C. Simionescu (1948–2024)*

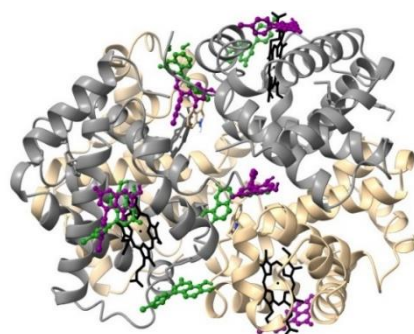
CONTROLLING THE BIOLOGICALLY RELEVANT REACTIVITY IN COUMARIN DERIVATIVES: FROM ANTIOXIDANT TO PROOXIDANT TO DNA TOXICITY IN TWO 5,7-DIHYDROXY-2H-CHROMEN-2-ONE DERIVATIVES

Nicoleta ANDRIAN, Cezara ZAGREAN-TUZA, Maria LEHENE, Balazs BREM, Emese GAL,
Bianca STOEAN, Luiza GAINA, Evamarie HEY-HAWKINS and Radu SILAGHI-DUMITRESCU*

Department of Chemistry, “Babeş-Bolyai” University, 11. Arany Janos, RO-400028 Cluj-Napoca, Roumania

Received February 28, 2025

In this study, we investigate the synthesis and biological reactivity of two structurally similar coumarin derivatives. Through a combination of experimental and computational approaches, we assess their interactions with key biomolecules such as calf thymus DNA, human serum albumin, and hemoglobin. Fluorescence quenching experiments and molecular docking simulations offer evidence for binding and explore possible binding sites. Redox assays demonstrate how both coumarin derivatives influence oxyhemoglobin autooxidation and modulate ferrylhemoglobin reactivity. Notably, a subtle structural variation between the two coumarins leads to significant differences in their antioxidant and prooxidant behaviors, as well as their interaction with DNA. One derivative exhibits stronger DNA binding and fragmentation effects, suggesting potential biomedical applications but also raising concerns about its genotoxic potential. These findings highlight the fine line between antioxidant and prooxidant reactivity and its implications for the development of therapeutic compounds.



INTRODUCTION

Plant-derived small aromatic molecules such as coumarins¹ are often cited for their biological activity and also used as starting points for the design of new therapeutics and/or theranostics.^{2,3} Long known for its anticoagulant properties, coumarin itself has also been shown to display other potentially useful biological activities – a fact which has sparked efforts to investigate a range of coumarin derivatives for their biomedically relevant and potentially therapeutic effects.^{1–4} Binding of

coumarin derivatives to a number of proteins – beginning with albumin but also including varied enzymes such as aromatases, cyclooxygenases and others, has been studied spectroscopically and followed up occasionally with biological studies.^{1–24} The antioxidant activity of coumarins, including those with 5,7-dihydroxy substitution patterns, has been explored extensively with standard tools such as DPPH radical scavenging, ABTS radical cation decolorization, and ferric reducing antioxidant power (FRAP) assays.^{1–3} Coumarins also interact with enzymes of the cytochrome P450 (CYP)

* Corresponding author: radu.silaghi@ubbcluj.ro

family such as CYP2A13 and CYP2A6, DNA polymerases, gyrases, or human carbonic anhydrases (CAs) such as CA IX and CA XII deemed as targets for cancer treatment. Cell assays aimed at exploring antimicrobial, antiproliferative, or antitumor potentials of coumarin derivatives were also explored.^{1–4,7–10,12,13,16,17,23–25}

The complex array of potential biological applications of coumarin derivatives has fuelled interest in development of synthesis strategies for new members of this class. The synthesis of coumarin derivatives has thus attracted significant interest, with novel procedures involving metal complexes as catalytic systems. The coumarin intramolecular ring closer starting from aryl alkynoates implies a hydroarylation reaction of a C≡C triple bond in the presence of platinum and palladium, and also rhodium metal complexes, namely Pt(OAc)₂, Pd(O₂CCF₃)₂(PPh₃)₂, and Pd(PPh₃)₄, Rh₂(OAc)₄,²¹ or more recently Pd(OAc)₂/Sc(OTf)₃.⁶ The gold derivatives, such as auric chloride, AuCl₃/3AgOTf,²⁶ and Au(PPh₃)Cl and AgSbF₆,²⁷ have also demonstrated significant catalytic activity. The classical synthesis of coumarin derivatives by Pechmann condensation of phenols or polyphenols with β-keto esters offers the advantages of a cheap, sulphuric acid catalyst and good yields.²³ This protocol remains in current use, facilitating the synthesis of novel coumarin derivatives, specifically 4-aryl-7-hydroxy-8-H-chromen-2-ones.²⁴ The sulphuric acid catalyst can be substituted with more environmentally friendly alternatives, such as zirconium phosphate,²⁸ or pyridinium ionic liquid,^{5,22} in all instances, the coumarin derivatives are obtained in satisfactory yields.

We have previously described the bidirectional redox reactivity of naturally occurring compounds typically considered as antioxidants. In most cases, such antioxidants (e.g., with vitamin C as the prime example) display two stable states – the ‘reduced’ (e.g., ascorbic acid) and the ‘two-electron oxidized’ (e.g., dehydroascorbic acid). Intermediate between the two, the one-electron reduced form (e.g., ascorbyl radical) can occur either through one-electron oxidation of the reduced form, or through comproportionation reactions between the reduced and the two-electron oxidized forms of the molecule. These radicals can subsequently suffer a second one-electron oxidation to a more stable form, or they can engage in varied reactions that may involve di/oligo/polymerizations, eliminations, couplings, oxidations, dehalogenations and others. We and others^{29–37} have shown for several natural compounds (ascorbate, coumarins, flavonoids, polyphenol, etc), as well as natural extracts, that large excesses of these ‘antioxidants’ can induce oxidative reactions very

similar to those induced by a classic biological reactive oxygen species (ROS), hydrogen peroxide. Moreover, we have developed a number of experimental methodologies to assess the prooxidant effect of biologically active compounds.^{29,31,38} For these, hemoglobin (Hb) is a convenient diagnostic tool in investigating the above-mentioned reactivities.³⁹ From the point of view of relevance, Hb’s large concentration in the blood implies inevitable contact with vitamins and antioxidants from food or from therapeutics. Hemoglobin’s iron center, via its multiple oxidation states (2+, 3+ and 4+ readily accessible under biologically relevant conditions) offers a range of redox reactions⁴⁰ that are susceptible to redox active interferents – for which we and others have described several analytical protocols. These reactions include:

(1) autooxidation of the oxy (ferrous-dioxygen) Hb to met (ferric) Hb. This parameter may be affected either via allosteric binding of the antioxidant to Hb (resulting in either acceleration or inhibition of autooxidation), or by reactions of the antioxidant with the superoxide (or its subsequent ROS products) liberated by oxy Hb upon autooxidation. The latter scenario may deplete the ROS and hence prevent an amplification cascade where ROS accelerate autooxidation by oxidizing the ferrous Hb, or the opposite – initiate chain reactions leading to more free radicals that may then degrade Hb and/or accelerate autooxidation

(2) autooxidation of oxy Hb in the presence of nitrite.⁴¹ This entails reactions similar to those described under item (1) above, except that reactive nitrogen species (RNS) are now also present in the solution (nitrite, nitrogen oxides, peroxyxynitrite and others).

(3) reaction with the high-valent Fe(IV) form of Hb. This species, known as Compound II by analogy with the catalytic cycles of heme-containing peroxidases, catalases, cytochrome P450 and others, features a ferryl unit at the heme and is easily generated *in vitro* as well as *in vivo* by reaction with hydrogen peroxide or with a range of other oxidizing agents – especially of the ROS family. The Hb Compound II can be reduced back to met Hb by antioxidants – and then the latter can in fact engage with Hb in a pseudoperoxidase reactivity with measurable Michaelis-Menten-type parameters. Alternatively, antioxidants can display modulatory (most often inhibitory) effects on the ascorbate pseudoperoxidase reactivity of Hb.

The goal of the present report is to explore and illustrate the degree to which subtle structural modifications can influence biomedically relevant reactivities in the coumarin class. For this, the

synthesis of two novel hydroxy 4-arylcoumarin derivatives, namely 4-(4-chlorophenyl)-5,7-dihydroxy-2H-chromen-2-one (**3a**) and 4-(4-chlorophenyl)-7,8-dihydroxy-2H-chromen-2-one (**3b**), has been accomplished through the utilisation of the Pechmann condensation, a method that has been proven to be both simple and efficient. The reactivity of these two compounds in Hb-related redox assays is then explored, alongside relatively standard albumin and hemoglobin binding assays. Since derivatives of this class are also known to affect cellular activity with implications on DNA functionality, the reactivity of our compounds is also explored against DNA. We find that a single relocation of an OH group on the coumarin ring, with only minor effects on the redox potential, has notable qualitative differences in prooxidant reactivity and in the reactivity towards DNA.

RESULTS AND DISCUSSION

The coumarin derivatives **3a** and **3b** were synthesized as previously described;¹³ compound **3a** has to our knowledge not been previously reported in the literature. Details on the synthesis and chemical characterization are given in the Experimental section. Compounds **3a** and **3b** were then subjected to a battery of tests, with results summarized in Table 1.

Figure 1 and Table 1 show that the two compounds, which are regioisomers of each other, are essentially degenerate in energy – with **3b** slightly more stable. The LUMO orbitals display similar shapes in the two compounds – with slightly more delocalization onto the 4-phenyl ring in the case of **3b**. This additional delocalization may be linked to the slightly lower energy (*i.e.*, stabilization) of the LUMO in **3b** compared to **3a** (by ~ 0.003 hartree) – and they can be proposed to originate from the different orientations of the two aromatic planes. Thus, the dihedral angle between the 4-phenyl group and the coumarin skeleton is 90.9° in **3a** and 56.6° in **3b** (*i.e.*, more conducive towards delocalization in the latter). No such differences are seen between the HOMO orbitals of the two isomers – either in energy or in spatial location. On the other hand, a clear difference is seen in the HOMO-1 orbitals – with **3b** showing contribution from one additional carbon atom within the coumarin skeleton, compared to **3a**; at the same time the **3b** HOMO-1 is ~ 0.01 higher in energy than its **3a** counterpart. Overall, the HOMO and especially the HOMO-1 orbitals of **3b** are slightly higher in energy than those of **3a**, suggesting that **3b** might be slightly more reactive as electron donor / antioxidant. These conclusions are in line with expectations as well as with previous analyses on the reactivity of dihydroxybenzene scaffolds: the two OH groups in **3a** are in a *meta* arrangement, known to be intrinsically less reactive than the *ortho* scaffold seen in **3b**.

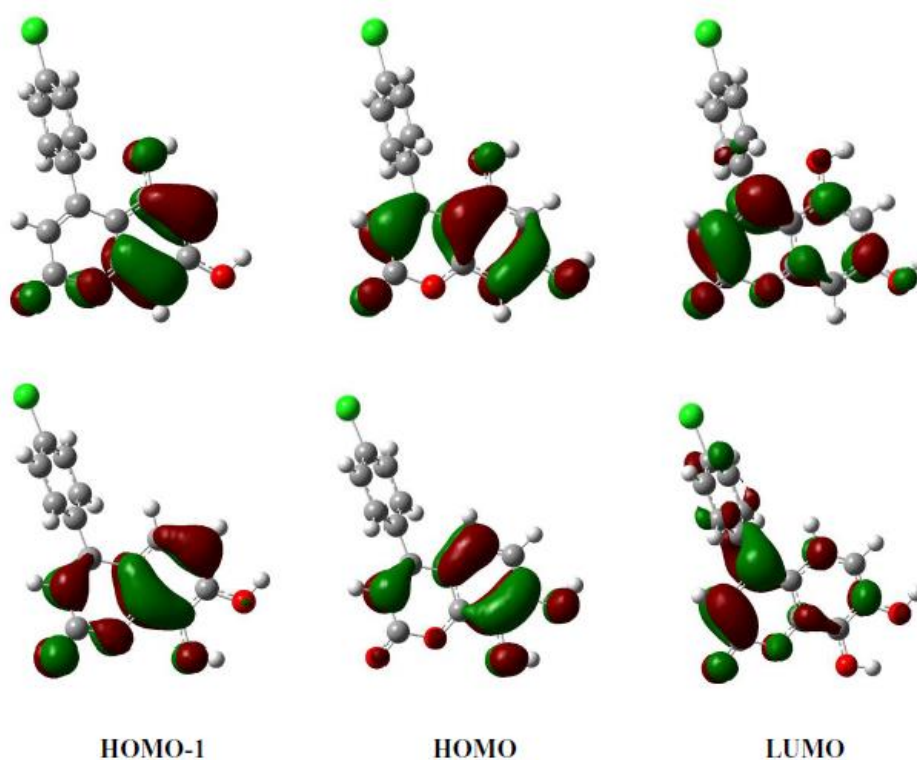


Fig. 1 – Structures and main frontier orbitals of **3a** (upper panel) and **3b** (lower panel) from DFT calculations.

Table 1

Summary of some theoretical and experimental parameters determined for compounds **3a** and **3b** in the present study

Compound		3a	3b	
DFT	Dipole moment	7.3	6.9	
	HOMO(-1) (a.u.)	-0.25341	-0.24342	
	HOMO (a.u.)	-0.23755	-0.23555	
	LUMO (a.u.)	-0.07274	-0.07868	
	HOMO-LUMO (a.u.)	-0.16481	-0.15687	
	LUMO-HOMO(-1) (a.u.)	0.18067	0.16474	
K _d docking [μ M]	HSA*	1	1	
	HSA	2	1	
	hHb	6	2	
	DNA	1	4	
K _d fluorescence [μ M]	K _d (BSA)	1.7	1.5	
	K _d (Hb)	55.4	21.2	
	K _d (DNA)	48	125	
Hb redox	Autooxidation rates of hemoglobin		0.1	0.2
	With nitrite	10 μ M	0.7	0.1
		1 μ M	0.1	0
Reactivity for Fe(IV)-Hb		0.7	0.8	

Binding to proteins

Figures 2 and 3 illustrate fluorescence experiments documenting the binding of **3a** and **3b** to albumin (BSA, bovine serum albumin) and to hemoglobin, while Table 1 lists the resulting calculated affinities. The fluorescence intensity at

330 nm was used in order to quantify the results; any intrinsic fluorescence (applicable for compound **3b**) was subtracted when the K_d was calculated. As can be seen in Table 1, the binding constants to albumin are much lower than to hemoglobin, indicating a higher affinity for the former.

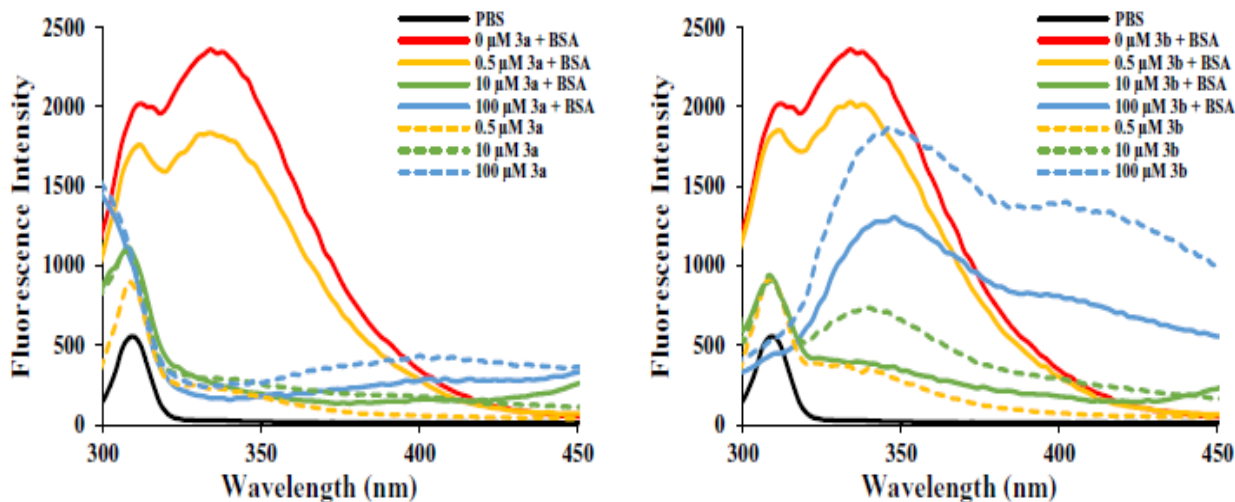


Fig. 2 – Fluorescence emission spectra collected with excitation at 280 nm for bovine serum albumin (BSA) in the presence of varying concentrations of compound **3a** and **3b**. Conditions PBS pH 7.4, room temperature, 0.15 μ M protein concentration.

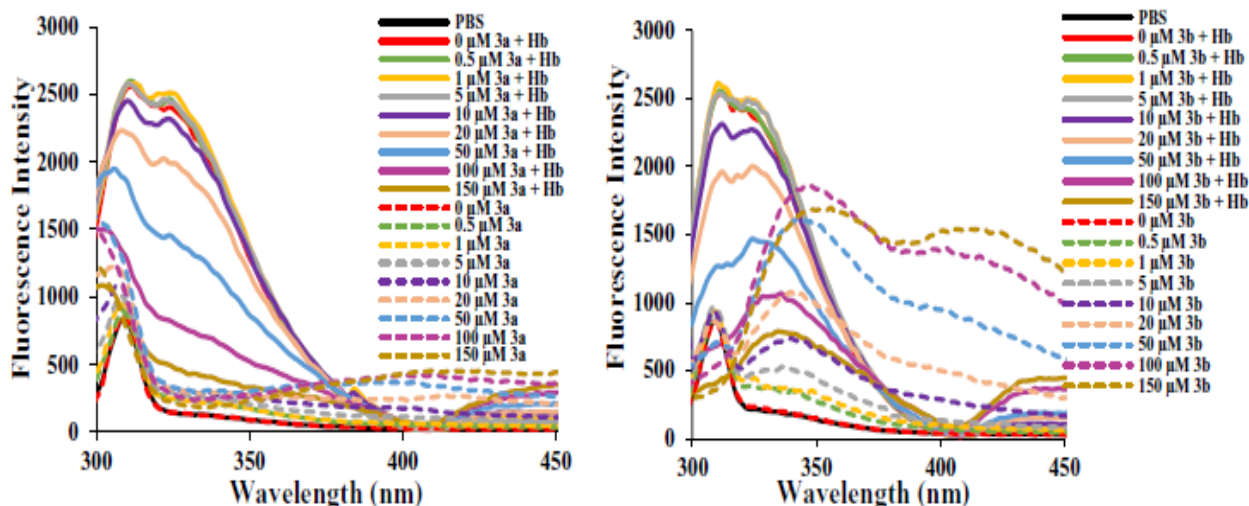


Fig. 3 – Fluorescence emission spectra collected with excitation at 280 nm for bovine serum hemoglobin (bHb) in the presence of varying concentrations of compound **3a** and **3b**. Conditions PBS pH 7.4, room temperature, 10 μ M protein concentration.

To gain more insight into the binding of the two coumarin derivatives, docking calculations were performed. These revealed a number of binding sites for **3a** and **3b** to human serum albumin (see Fig. 4 and Table 1). Both molecules bind to approximately the same regions of the protein due to their structural similarities. Two of the binding sites comprise aromatic aminoacids, Tyr148, Tyr150 and Tyr204, which explains the decrease in fluorescence upon the addition of coumarin derivatives. The computed affinities for the two compounds are at 1-2 μ M cf. Table 1, in good agreement with the experimental binding constants deduced from our fluorescence measurements (1.7 μ M for **3a** and 1.5 μ M for **3b**). The low-micromolar affinities of these two compounds for albumin as a representative protein are in line with previous reports on related 6,7-dihydroxycoumarin derivatives found to have similarly low-micromolar affinities for the oncoprotein Mcl-1 (induced myeloid leukemia cell differentiation protein Mcl-1) mirrored by similar IC_{50} values in Mcl-1 cells.⁴² Similar low-micromolar IC_{50} values were derived for a series of 5,7-dihydroxy-4-propyl-chromen-2-one derivatives on four cancer lines.¹⁷ Derivatives such as 4-(chloromethyl)-5,7-dihydroxy-2H-chromen-2-one, 4-((acetylthio)methyl)-2-oxo-2H-chromen-7-yl acetate, 4-(chloromethyl)-7,8-dihydroxy-2H-chromen-2-one, 7-(2-(oxiran-2-yl)ethoxy)-2H-chromen-2-one and 7-(3-(oxiran-2-yl)propoxy)-2H-chromen-2-one also displayed low-

micromolar affinities for a number of targets (DNA polymerase, tumor cell lines, anti-retroviral activity).¹⁶ The binding of coumarin derivatives to serum albumin itself has previously been described rather incompletely in terms of docking calculations. For instance reference⁴³ lists only the highest-affinity binding site, without discussing alternatives – while our own study here suggests multiple binding sites of similar affinity, of which the site located at the center of the albumin structure in Fig. 4 does indeed coincide with the site identified in reference⁴³ as well as in reference⁴⁴ (as site FA8) for other coumarin derivatives. The other two sites presented in Fig. 4 mirror heme-binding sites previously identified in serum albumin.⁴⁴ Reference⁴⁵ on the other hand does identify several binding sites for coumarin derivatives (7-hydroxy), distributed around aromatic aminoacids and potentially responsible for the ability of a number of coumarin derivatives. Examples of such derivatives were 4-hydroxycoumarin, 8-acetyl-7-hydroxycoumarin, 4-methyl-7-hydroxy-8-(3-chlorobenzoyl)coumarin, 4-methyl-7-hydroxy-6-(3-chlorobenzoyl)coumarin, 4-benzo [1,3]dioxol-5-yloxymethyl)-7-hydroxy-chromen-2-one. For these compounds, it was pointed out that the position of the hydroxyl group and the presence of different non-polar moieties does not change the fluorescence quenching mechanism. This is in line with the similarities we find in binding sites and affinities for our compounds, **3a** and **3b**.

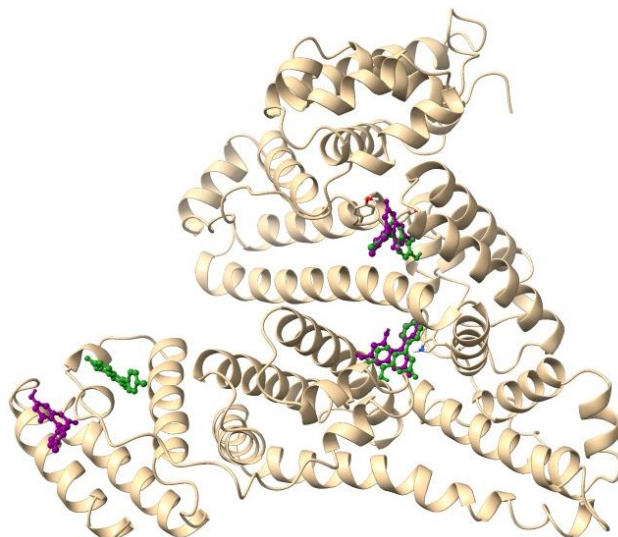


Fig. 4 – Highest-affinity binding sites of coumarin derivatives **3a** (purple) and **3b** (green) to human serum albumin (pdb code: 1gnj⁴⁶).

The two compounds share very similar binding sites in human hemoglobin as well; the results are illustrated in Fig. 5 and Table 1. The highest affinity was calculated for conformations in the vicinity of Trp37, which explains the decrease in fluorescence when each molecule is added to the protein. Compound **3b** exhibited a higher average affinity; however, the difference in affinity is not necessarily significant (2 μM versus 6 μM). Moreover, both compounds can bind in the vicinity of the heme, more precisely through contacts with the heme propionate group. More conformations seem to be possible for both molecules. Heme-bound **3b** conformations do exhibit higher affinities (18–78 μM), as opposed to the corresponding **3a** conformers (57–134 μM). This difference in affinity when interacting with the

propionate group could influence the slightly higher autooxidation rate and reactivity towards ferrylhemoglobin observed in **3b** compared to **3a** (vide infra) – the higher the binding affinity to the propionate group, the better the electron transfer. It is perhaps of interest to note that the affinities computed for Hb in our docking calculations, as well as the affinities derived from fluorescence experiments, are both ~one order of magnitude weaker than those computed for albumin. This observation validates the docking calculations in their ability to predict trends aligned with experiments. One may also note that Hb's less efficient binding is in line with the fact that serum albumin is designed to be a transport protein – hence with built-in capability for versatile and efficient ligand binding – unlike Hb.

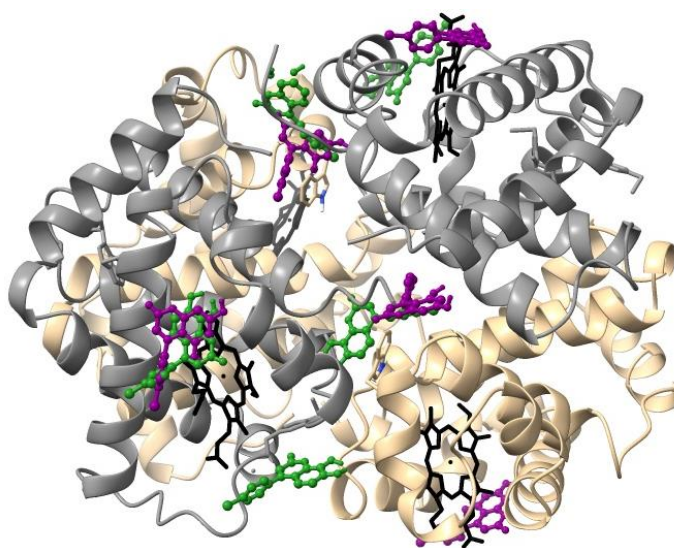


Fig. 5 – Highest-affinity binding sites of coumarin derivatives **3a** (purple) and **3b** (green) to human hemoglobin (pdb code: 1mko⁴⁷). Binding sites in contact with the heme (black) are also shown.

Redox reactivity

Figure 6 illustrates the UV-vis spectra collected during the reaction of ferryl (Fe(IV)) Hb with **3a** and **3b** over the course of 15 minutes, together with control samples. The positive control is ascorbate, known to efficiently reduce ferryl Hb; the negative control is ferryl Hb with no added reducing agent. Both of our coumarin derivatives reduce the high-valent form of Hb slightly less efficiently than ascorbate. Table 1 gives a quantitative measure: the values listed for the ferryl measurements are fractional numbers based on the absorbance changes at 580 nm and

630 nm after the first 15 minutes and normalized so that 0.0 would correspond to no reduction of ferryl and 1.0 would correspond to the same degree of reduction of ferryl as afforded by our reference antioxidant, ascorbate. The indices shown in Table 1 imply that **3a** and **3b** are able to reduce ferryl Hb 70-80% as effectively as ascorbate – with the slightly higher value (0.8) in the case of **3b**. The latter difference between the two compounds is in good agreement with the above-discussed predictions made from DFT calculations and from basic structural considerations (*ortho*- vs. *meta*) according to which **3b** was expected to be more reactive.

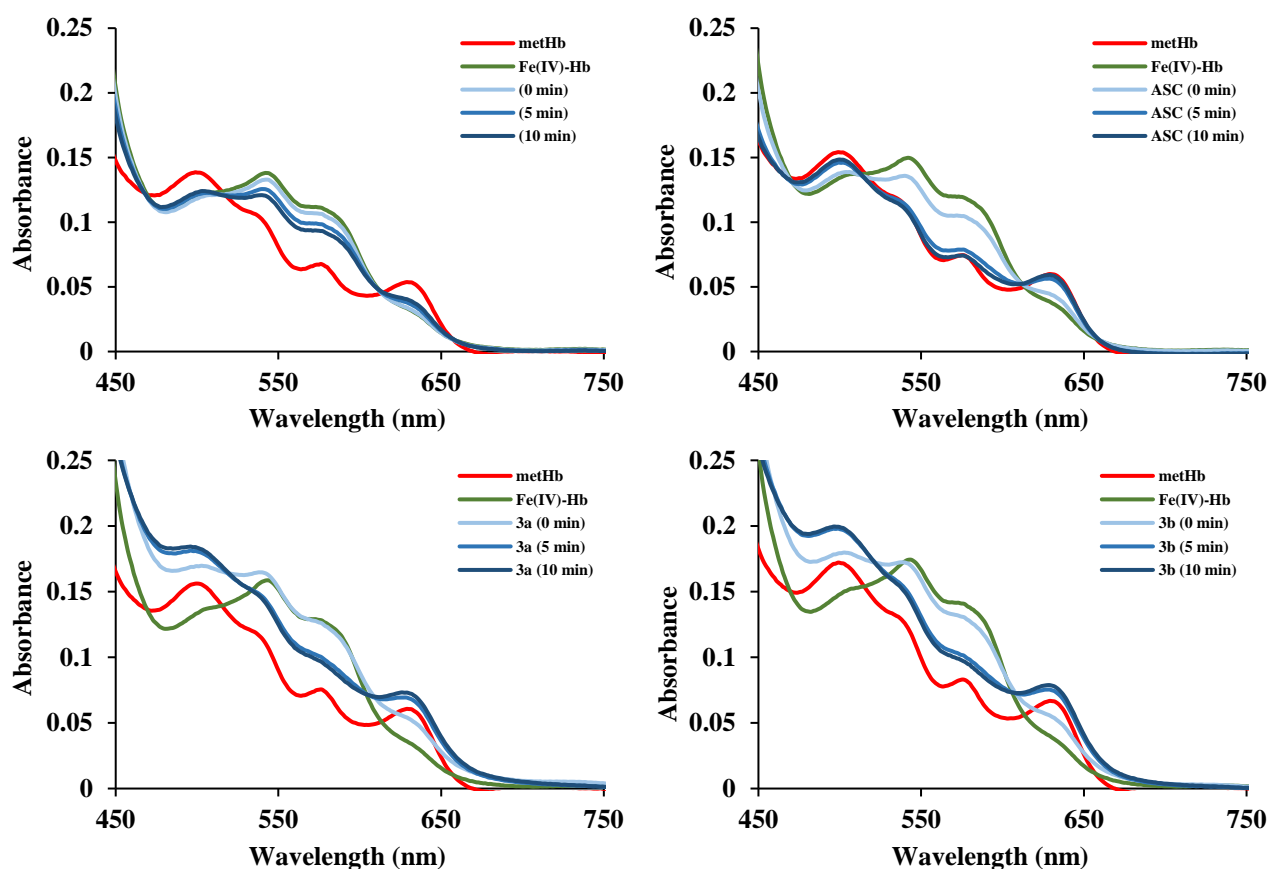


Fig. 6 – UV-vis spectra of 15 μM Fe(IV)-Hb in the presence of 150 μM of **3a** and **3b** in PBS buffer pH 7.4 at room temperature.

Figure 7 shows the behavior of oxy (ferrous-dioxygen Hb) in the presence of **3a** and **3b**, compared against control experiments with DMSO since the two compounds are added as stock solutions in this solvent. Table 1 offers a quantification of this data, again based on normalized values as in the case of the ferryl reactivity. The values, 0.1 for **3a** and 0.2 for **3b**, imply a very small degree (10–20%) of acceleration

of the autooxidation reaction – *i.e.*, a slight prooxidant reactivity – and slightly higher for **3b** than for **3a**. The improved delocalization of electrons in **3b**, evidenced from the DFT calculations discussed above, may imply a slightly increased stability of the free radicals generated upon oxidation of **3a** or **3b** and hence more chances for those radicals to engage in further oxidative damage.

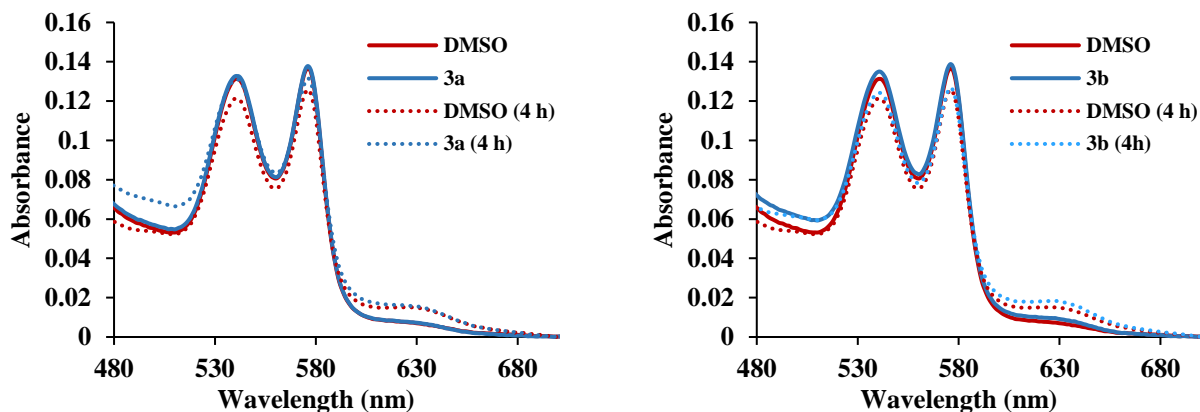


Fig. 7 – UV-vis spectra of 10 μM oxy Hb in the presence of 100 μM of **3a** and **3b**, before and after incubation for 4 hours at 37°C in PBS buffer pH 7.4. Control experiments in DMSO are also shown.

Figure 8 illustrates the time course of the autooxidation reaction of oxy Hb, this time in the presence of nitrite. As previously shown in detail, this reaction mixture leads to autocatalytic processes where reactive oxygen species and reactive nitrogen species accelerate the oxidation of the heme and eventually lead to its degradation. Small molecules are known to be able to interfere with this process mainly by reacting with these ROS or RNS – either quenching them or amplifying their reactivity. Compound **3a** shows the expected concentration-dependent antioxidant behavior, slowing down the oxidation

process at concentrations of 1 and of 10 μM but not at 0.1 μM . In contrast, **3b** shows a slight accelerating effect at 10 μM – *i.e.*, a slight prooxidant effect. It is in principle well accepted that antioxidant and prooxidant activities may both manifest in the same compounds, and that they do not necessarily correlate^{30,38,48} – as they depend to differing degrees on redox potential, hydrophobicity, routes towards final products subsequent to the initial one-electron reaction, ability to bind to given targets, and involvement of different sets of frontier molecular orbitals.

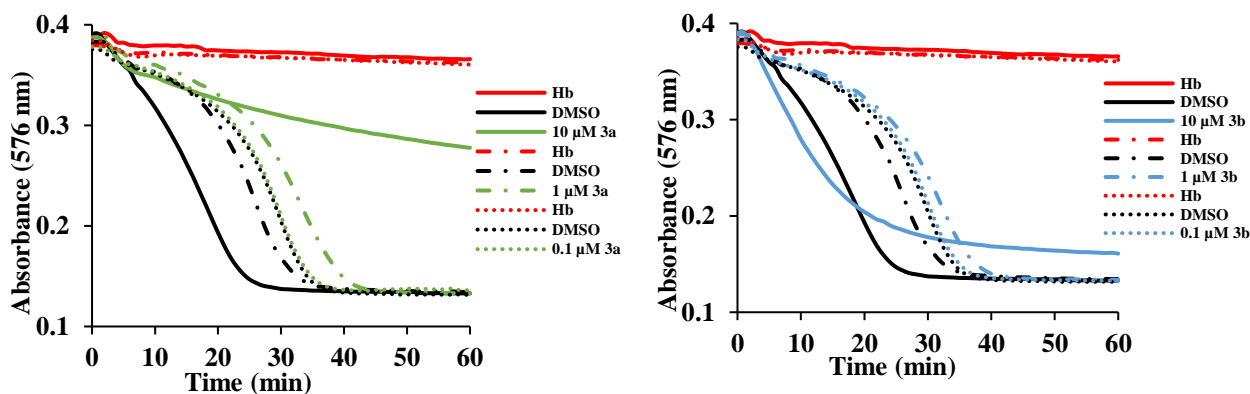


Fig. 8 – Time course of nitrite oxidation of hemoglobin in phosphate-buffered saline (PBS) at 240 μM nitrite and various compound concentrations. Conditions: 30 μM oxy Hb, PBS 7.4, room temperature.

Interaction with DNA

The interaction of the compounds with calf thymus DNA was analyzed in a displacement assay using the SYBR GREEN dye. Both the dye and the calf thymus DNA have no intrinsic fluorescence individually. Binding of the dye to DNA causes fluorescence with excitation at 495 nm and emission at 520 nm. The decay of this

fluorescence was monitored as a result of the interaction of ligands with calf thymus DNA. Compounds **3a** and **3b** have no intrinsic fluorescence with excitation at 495 nm and emission at 520 nm, and did induce concentration-dependent decreases in fluorescence of the DNA/SYBR GREEN system. Table 1 shows the calculated affinities – with **3a** binding somewhat (x5) better than **3b** to calf thymus DNA.

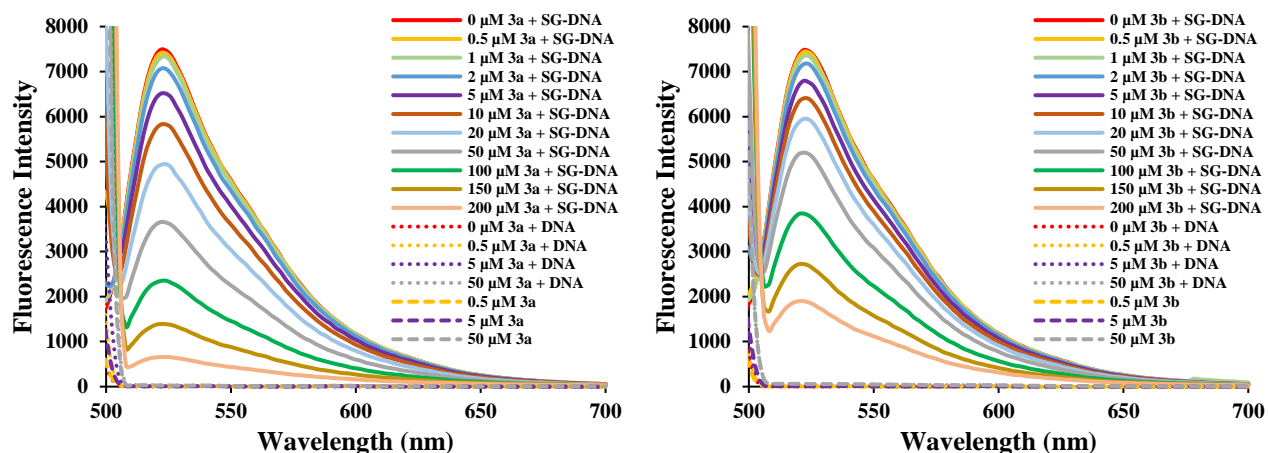


Fig. 9 – Fluorescence emission spectra collected with excitation at 495 nm for 2 μ M calf thymus DNA with SYBR GREEN in presence of varying concentrations of compound **3a** and **3b** in Tris-HCl buffer pH 7.4, at room temperature. Ligand concentrations are indicated in Figure legends.

Figure 10 shows the effect of **3a** and of **3b** on plasmid DNA, as measured using gel electrophoresis. Cisplatin is included as positive control, with the expected effect – the DNA is degraded and displays the typical ladder-like pattern as smaller and smaller fragments are generated. Also included as control is a Pt(IV) complex, oxoplatin. Although smaller, its effect appears similar to that of cisplatin with one observation: the plasmid migrates according to an apparent higher molecular weight, suggesting that oxoplatin has bound to the plasmid under these conditions but has not been as efficient as cisplatin in cleaving it. Compound **3b** displays, similarly to oxoplatin, a higher apparent mass for the plasmid. This effect is by far more significant for compound **3a** – where not only do we see a higher-mass band, but also see most of the plasmid at a mass shifted to significantly lower values. The distinctly stronger effect of **3a**

compared to **3b** in the gel assay correlates well with the higher affinity seen for the **3a**-DNA interaction in the fluorescence assay but, instructively of not somewhat expectedly, does not correlate with the redox ability explored in the previous sections of this report.

Also shown in Figure 10 are the results of DNA docking calculations, which support the concept of **3a** and **3b** binding to DNA with affinities in the micromolar range – *i.e.*, with potential biomedical relevance. The binding is proposed to occur in the minor groove of the DNA.

Some coumarin derivatives were previously shown to bind to DNA and alter it – though to our knowledge a detailed structural exploration of the binding phenomena is not available. These previously identified affinities were in the same range as the numbers reported from our fluorescence experiments in Table 1.^{15,16}

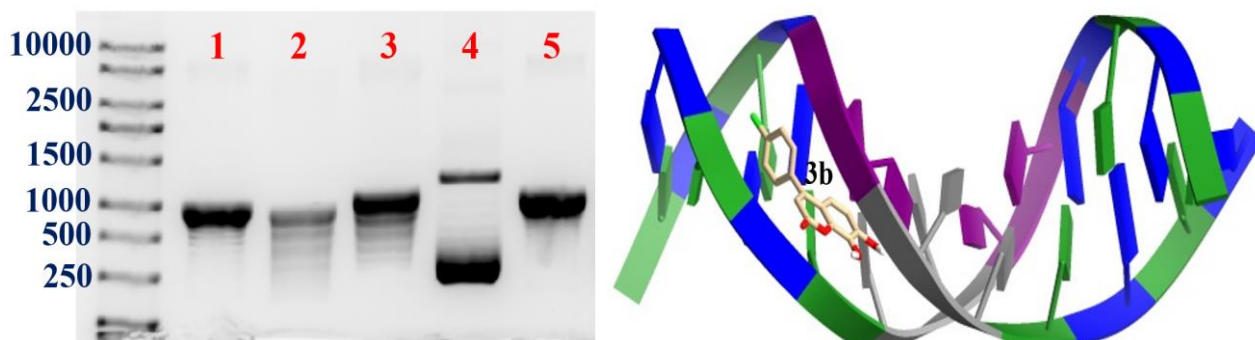


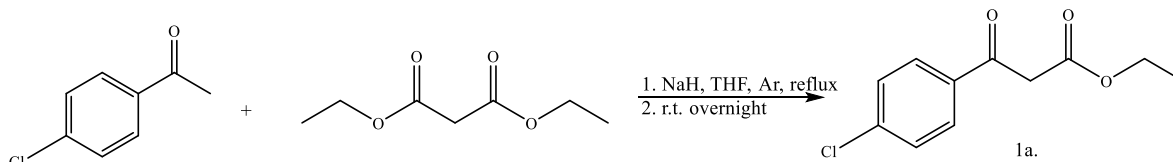
Fig. 10 – **Left:** pUC19 plasmid treated with 1- DMSO; 2- cisplatin; 3- oxoplatin; 4- coumarin derivative **3a**, and 5- coumarin derivative **3b** analyzed on a 1% agarose gel. The DNA ladder (on the left) is in base pairs. **Left:** Binding site of coumarin derivative **3b** to a DNA fragment (pdb code: 1bna⁴⁹) in the small groove. Adenine in purple, cytosine in green, guanine in blue and thymine in grey. The calculated affinity is 1 μ M for **3a** and 4 μ M for **3b**.

EXPERIMENTAL

The structures of the synthesized 4-phenylcoumarins **3a** and **3b** were confirmed based on nuclear magnetic spectroscopy (NMR) and high-resolution mass spectrometry (HRMS). HRMS were performed on Thermo Scientific LTQ Orbitrap XL mass spectrometer ESI in positive ionization mode. The nuclear magnetic resonance (NMR) spectra were recorded on a Bruker Avance spectrometer (400 MHz).

Synthesis of compound ethyl 3-(4-chlorophenyl)-3-oxopropanoate

A flame-dried, three-necked 250 mL flask equipped with a magnetic stirrer was charged with



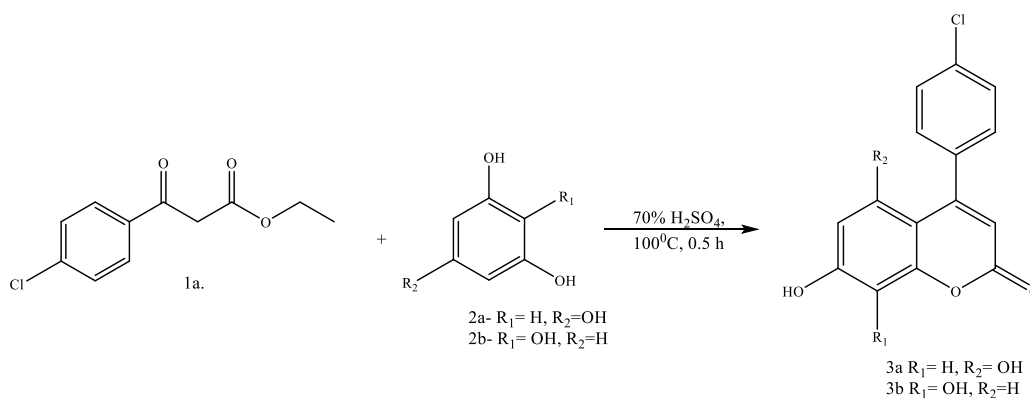
1a ^1H NMR 400 MHz CDCl_3 δ ppm: 1.18 (t, 3H, CH_3), 3.91 (s, 2H, CH_2), 4.13 (q, 2H, O- CH_2), 7.37 (d, 2 H, $^3J = 7.90$ Hz), 7.81 (d, 2 H, $^3J = 7.90$ Hz)

1a ^{13}C NMR 100 MHz CDCl_3 δ ppm: 13.9 (CH_3), 45.8 (CH_2), 61.5 (O- CH_2), 129.0 (2 CH), 129.8 (2 CH), 134.2 (C), 140.1 (C), 167.2 (-COO-), (C), 191.3 (C=O)

HRMS calc. For $\text{C}_{11}\text{H}_{11}\text{ClO}_3$ 226.0396/228.03674, measured (APCI +) for $[\text{C}_{11}\text{H}_{11}\text{ClO}_3+\text{H}]$ $[\text{M}+\text{H}]$ 227.0474/229.0442.

General procedure for the synthesis of compounds **3a** and **3b**, **Pechmann reaction**:¹³ Resorcin (**2a**) or phloroglucinol (**2b**) (1.0 g, 7.93 mmol), (1.0 g, 9.09 mmol), ethyl 3-(4-chlorophenyl)-3-oxopropanoate **1a**, (1.74 g, 9.09 mmol), and 70% H_2SO_4 (15 ml) were combined and stirred at room temperature for 12 hours. Following the reaction completion, the mixture

was subjected to a work-up procedure involving quenching with crushed ice, followed by two successive extractions with 25 mL portions of ethyl acetate. Removal of the solvent by evaporation resulted in a brown solid. This solid was then subjected to recrystallization from methanol, leading to the isolation of a yellowish compound **3a** and **3b**.



3a ^1H NMR 600 MHz $\text{DMSO}-d_6$ δ ppm: 5.77 (s, 1H, CH), 6.16 (d, 1H, CH , $^4J = 2.20$ Hz), 6.27 (d, 1H, CH , $^4J = 2.20$ Hz), 7.35 (d, 2 H, CH , $^3J = 8.50$ Hz), 7.41 (d, 2 H, CH , $^3J = 8.50$ Hz), 7.86 (d, 1 H, CH , $^3J = 8.70$ Hz), 10.79 (s, 1H, OH)

3a ^{13}C NMR 125 MHz $\text{DMSO}-d_6$ δ ppm: 94.6 (CH), 99.1 (CH), 100.4 (CH), 110.3 (C), 127.3 (2 CH), 129.4 (2 CH), 132.6 (C), 138.4 (C), 154.7 (C), 156.7 (C), 159.8 (C), 161.9 (C), 170.4 (C=O)

HRMS calc. For $\text{C}_{15}\text{H}_9\text{ClO}_4$ 288.0189/290.0160, measured (APCI+) for $[\text{C}_{15}\text{H}_9\text{ClO}_4+\text{H}]$ $[\text{M}+\text{H}]$ 289.0267/291.0238

3b ¹H NMR 600 MHz DMSO-*d*₆ δ ppm: 5.77 (s, 1H, CH), 6.15 (d, 1H, CH, ⁴*J* = 2.26 Hz), 6.27 (d, 1H, CH, ⁴*J* = 2.26 Hz), 7.35 (d, 2H, CH, ³*J* = 8.00 Hz), 7.42 (d, 2H, CH, ³*J* = 8.00 Hz), 7.86 (d, 1H, CH, ³*J* = 8.70 Hz), 10.26 (s, 1H, OH)
3b ¹³C NMR 125 MHz DMSO-*d*₆ δ ppm: 94.8 (CH), 99.2 (CH), 110.3 (C), 127.4 (2 CH), 129.5 (2 CH), 132.7 (C), 138.4 (C), 156.8 (C), 157.1 (C), 159.9 (C), 161.9 (C), 171.4 (C=O)
HRMS calc. For C₁₅H₉ClO₄ 288.0189/290.0160, measured (APCI+) for [C₁₅H₉ClO₄+H] [M+H] 289.0243/291.0225

UV-vis spectra were recorded on a Lambda 25 (PerkinElmer Singapore) spectrophotometer. Native bovine Hb was purified according to literature procedures⁵⁰ and converted into the oxy form by treatment with dithionite (and into the met form by treatment with potassium ferrocyanide) followed by a desalting step. Bovine serum albumin (BSA, from Sigma-Aldrich, Schnellendorf, Germany) was used as provided without further purification. Protein stock solutions were prepared in phosphate buffer saline (PBS). Concentrations are given per heme in the case of Hb and per monomer for the rest of proteins. Other reagents used are as follows: sodium nitrite (NaNO₂, Reactivul Bucuresti, Bucharest, Romania), L-ascorbic acid (Sigma-Aldrich, Schnellendorf, Germany).

For the reaction with the high-valent Fe(IV) Hb, 15 μM met Hb were treated with hydrogen peroxide, followed by the addition of 150 μM compound. The spectra were recorded at 0, 5, 10 and 15 min.

For the autoxidation reaction, 10 μM oxy Hb were mixed with 100 μM from each compound. The spectra were recorded before and after 4 h incubation at 37°C.

The kinetic of the autoxidation reaction of oxy Hb in the presence of nitrite was monitored with a Spark 10M microplate reader (Tecan GmbH, GrödigM Austria). To prepare samples, 30 μM of oxy Hb were mixed with 240 μM NaNO₂ and different concentrations from each compound.

Fluorescence spectra were recorded using a SpectroFluoroPhotoMeter RF-6000 (A40245400634SA). For each fluorescence test, 10 μM met Hb or 0.15 μM bovine serum albumin were treated with different concentrations from each coumarin derivative. For albumin experiments, individual samples were prepared for each concentration, whereas classic titration was performed for Hb binding determination. Since Compounds **3a** and **3b** were employed as a stock solution in DMSO, control spectra were also collected illustrating the lack of effect of DMSO at the employed concentrations/volumes (not shown).

For the DNA assays, 9 nM pUC19 plasmid (from Roth, 25 μg/mL from) were incubated with 90 nM cisplatin, oxoplatin, and coumarin derivatives **3a** and **3b**, respectively, together with the fluorescent dye SYBR GREEN for four hours. Bromophenol

blue was added to each sample, which were subsequently loaded on a 1% agarose gel. The gel was analyzed with a fluorescent imager, with the excitation wavelength 495 nm.

For DFT calculations, the Gaussian16⁵¹ software package was employed. The **3a** and **3b** structures were computed with the B3LYP^{52,53} functional at the def2-SV(P)⁵⁴ double-zeta basis set level. The DFT-optimized structures were loaded in the AutoDock Tools⁵⁵ package and prepared for molecular docking, together with human hemoglobin (pdb code: 1mko⁴⁷) and human serum albumin (pdb code: 1gnj⁴⁶) as receptors. Human serum albumin was used in two forms as receptor: in complex with five molecules of arachidonic acid (HSA*) and free (without any other bound molecule). For blind docking, a grid box with 126×126×124 dimensions was used for both receptors, with 0.7 Å spacing. Other docking calculations were performed with a DNA fragment (pdb code: 1bna⁴⁹) as receptor, with a grid box of 68×82×118 and 0.4 Å spacing. The dockings were performed through the Genetic Algorithm (GA), with default parameters and 100 runs. The docking calculations were performed with Autodock4 and the results were analyzed were analyzed in Autodock Tools and ChimeraX.

Data supporting the present report (DFT and docking outputs) are available freely online as Andrian, Nicoleta; Zagrean-Tuza, Cezara; Lehene, Maria; Silaghi-Dumitrescu, Radu (2025), "Data for: Controlling the biologically-relevant reactivity in coumarin derivatives: from antioxidant to prooxidant to DNA toxicity, by Andrian *et al.*", "Babeş-Bolyai" University, V1, doi: 10.17632/kvbhc8yr2g.1 .

CONCLUSIONS

We have reported here the synthesis of two coumarin derivatives, regioisomers and one of which, **3a**, is to our knowledge not previously reported in the literature. We have characterized their binding and redox reactivity with proteins, rationalizing the results with the use of DFT and of docking calculations. The expected antioxidant reactivity of **3a** and **3b** is found to be mirrored by a

concentration-dependent prooxidant reactivity especially in the presence of reactive nitrogen species – but only for one of the two isomers. Both compounds bind to DNA, with **3a** not only binding more efficiently but also showing distinct degradation of plasmid DNA – more so than cisplatin. These findings suggest potential biomedical applications towards development of new cytostatic treatments. On the other hand, the nature-inspired structures of the two compounds also points out to an important consideration about the potential of naturally occurring (as well as of synthetic ones) compounds and antioxidants to degrade DNA in general – *i.e.*, to act as genotoxic rather than protective molecules.

Acknowledgements. Support from the project “Targeted Tumor Therapy with multifunctional platinum(IV)-drug conjugates, T3-Pt”, PNRR-III-C9-2023-I8-CF76, contract no. 760240/28.12.2023 funded by the European Union – NextGenerationEU and the Roumanian Government, under the National Recovery and Resilience Plan for Romania, through the Roumanian Ministry of Research, Innovation and Digitalization, within Component 9, Investment I8 is gratefully acknowledged. Dr. Madalina Moisa (from the Enzymology and Applied Biocatalysis Research Center) and Dr. Adrian Branzanic from Babes-Bolyai University are acknowledged for useful discussions.

REFERENCES

- Kostova, I.; Bhatia, S.; Grigorov, P.; Balkansky, S.; S. Parmar, V.; K. Prasad, A.; Saso, L., *Curr. Med. Chem.* **2011**, *18*, 3929–3951. <https://doi.org/10.2174/092986711803414395>.
- Flores-Morales, V.; Villasana-Ruíz, A. P.; Garza-Veloz, I.; González-Delgado, S.; Martínez-Fierro, M. L., *Molecules* **2023**, *28*, 2413. <https://doi.org/10.3390/molecules28052413>.
- Todorov, L.; Saso, L.; Kostova, I., *Pharmaceuticals* **2023**, *16*, 651. <https://doi.org/10.3390/PH16050651>.
- Sharifi-Rad, J.; Cruz-Martins, N.; López-Jornet, P.; Lopez, E. P. F.; Harun, N.; Yeskaliyeva, B.; Beyatli, A.; Sytar, O.; Shaheen, S.; Sharopov, F.; Taheri, Y.; Docea, A. O.; Calina, D.; Cho, W. C., *Oxid. Med. Cell. Longev.* **2021**, *2021*, 6492346. <https://doi.org/10.1155/2021/6492346>.
- Uroos, M.; Javaid, A.; Bashir, A.; Tariq, J.; Khan, I. H.; Naz, S.; Fatima, S.; Sultan, M., *RSC Adv.* **2022**, *12*, 23963–23972. <https://doi.org/10.1039/D2RA03774B>.
- Dong, S.; Li, K.; Li, S.; Chen, Z.; Yin, G., *ChemistrySelect* **2024**, *9*, e202401710. <https://doi.org/10.1002/slct.202401710>.
- Von Weymarn, L. B.; Chun, J. A.; Knudsen, G. A.; Hollenberg, P. F., *Chem. Res. Toxicol.* **2007**, *20*, 1252–1259. <https://doi.org/10.1021/tx700078v>.
- Shimada, T.; Kim, D.; Murayama, N.; Tanaka, K.; Takenaka, S.; Nagy, L. D.; Folkman, L. M.; Foroozesh, M. K.; Komori, M.; Yamazaki, H.; Guengerich, F. P., *Chem. Res. Toxicol.* **2013**, *26*, 517–528. <https://doi.org/10.1021/tx300492j>.
- Shimada, T.; Murayama, N.; Tanaka, K.; Takenaka, S.; Guengerich, F. P.; Yamazaki, H.; Komori, M., *Chem. Res. Toxicol.* **2011**, *24*, 1327–1337. <https://doi.org/10.1021/tx200218u>.
- Su, T.; Bao, Z.; Zhang, Q. Y.; Smith, T. J.; Hong, J. Y.; Ding, X., *Cancer Res.* **2000**, *60*, 5074–5079.
- Shimada, T.; Takenaka, S.; Kakimoto, K.; Murayama, N.; Lim, Y. R.; Kim, D.; Foroozesh, M. K.; Yamazaki, H.; Guengerich, F. P.; Komori, M., *Chem. Res. Toxicol.* **2016**, *29*, 1029–1040. <https://doi.org/10.1021/acs.chemrestox.6b00083>.
- Von Weymarn, L. B.; Zhang, Q. Y.; Ding, X.; Hollenberg, P. F., *Carcinogenesis* **2005**, *26*, 621–629. <https://doi.org/10.1093/carcin/bgh348>.
- Olmedo, D.; López-Pérez, J.; Del Olmo, E.; Bedoya, L.; Sancho, R.; Alcamí, J.; Muñoz, E.; Feliciano, A.; Gupta, M., *Molecules* **2017**, *22*, 321. <https://doi.org/10.3390/molecules22020321>.
- Shimada, T.; Murayama, N.; Yamazaki, H.; Tanaka, K.; Takenaka, S.; Komori, M.; Kim, D.; Guengerich, F. P., *Chem. Res. Toxicol.* **2013**, *26*, 529–537. <https://doi.org/10.1021/tx3004906>.
- Xia, Y. L.; Wang, J. J.; Li, S. Y.; Liu, Y.; Gonzalez, F. J.; Wang, P.; Ge, G. B., *Bioorg. Med. Chem.* **2021**, *29*, 115851. <https://doi.org/10.1016/J.BMC.2020.115851>.
- Bruna-Haupt, E. F.; Perretti, M. D.; Garro, H. A.; Carrillo, R.; Machín, F.; Lorenzo-Castrillejo, I.; Gutiérrez, L.; Vega-Hissi, E. G.; Mamberto, M.; Menacho-Marquez, M.; Fernández, C. O.; García, C.; Pungitore, C. R., *ACS Omega* **2023**, *8*, 26479–26496. <https://doi.org/10.1021/ACSOMEGA.3C03181>.
- Abd-El-Aziz, A. S.; Alsaggaf, A. T.; Okasha, R. M.; Ahmed, H. E. A.; Bissessur, R.; Abdelghani, A. A.; Afifi, T. H., *ChemistrySelect* **2016**, *1*, 5025–5033. <https://doi.org/10.1002/SLCT.201600789>.
- Gümüş, A.; Karadeniz, Ş.; Uğraş, H. I.; Bulut, M.; Çakir, Ü.; Gören, A. C., *J. Heterocycl. Chem.* **2010**, *47*, 1127–1133. <https://doi.org/10.1002/JHET.435>.
- Fukami, T.; Katoh, M.; Yamazaki, H.; Yokoi, T.; Nakajima, M., *Chem. Res. Toxicol.* **2008**, *21*, 720–725. <https://doi.org/10.1021/tx700325f>.
- Shimada, T.; Takenaka, S.; Murayama, N.; Yamazaki, H.; Kim, J. H.; Kim, D.; Yoshimoto, F. K.; Guengerich, F. P.; Komori, M., *Chem. Res. Toxicol.* **2016**, *28*, 268–278. <https://doi.org/10.1021/tx500505y>.
- Jia, C.; Piao, D.; Kitamura, T.; Fujiwara, Y., *J. Org. Chem.* **2000**, *65*, 7516–7522. <https://doi.org/10.1021/jo000861q>.
- Rajabi, F.; Voskressensky, L. G.; Luque, R., *J. Organomet. Chem.* **2024**, *1022*, 1–7. <https://doi.org/10.1016/j.jorganchem.2024.123388>.
- Ranjitha, N.; Krishnamurthy, G.; Bhojya Naik, H. S.; Pari, M.; Anil Kumar, H. A.; Akarsh, G. Y.; Vasantakumarnaik, N. K., *Polyhedron* **2024**, *253*, 116909. <https://doi.org/10.1016/j.poly.2024.116909>.
- De Luca, L.; Mancuso, F.; Ferro, S.; Buemi, M. R.; Angeli, A.; Del Prete, S.; Capasso, C.; Supuran, C. T.; Gitto, R., *Eur. J. Med. Chem.* **2018**, *143*, 276–282. <https://doi.org/10.1016/j.ejmech.2017.11.061>.
- Henriquez-Figueroa, A.; Morán-Serradilla, C.; Angulo-Elizari, E.; Sanmartín, C.; Plano, D., *Eur. J. Med. Chem.*, **2023**, *246*, 115002. <https://doi.org/10.1016/J.EJMECH.2022.115002>.
- Shi, Z.; He, C., *J. Org. Chem.*, **2004**, *69*, 3669–3671. <https://doi.org/10.1021/jo0497353>.
- Aparece, M. D.; Vadola, P. A., *Org. Lett.* **2014**, *16*, 6008–6011. <https://doi.org/10.1021/ol503022h>.
- Sinhamahapatra, A.; Sutradhar, N.; Pahari, S.; Bajaj, H. C.; Panda, A. B., *Appl. Catal. A Gen.*, **2011**, *394*, 93–100. <https://doi.org/10.1016/j.apcata.2010.12.027>.

29. Mot, A. C.; Damian, G.; Sarbu, C.; Silaghi-Dumitrescu, R., *Redox Rep.* **2009**, *14*, 267–274. <https://doi.org/10.1179/135100009X12525712409814>.
30. Farcas, A. D.; Mot, A. C.; Zagrean-Tuza, C.; Toma, V.; Cimpoi, C.; Hosu, A.; Parvu, M.; Roman, I.; Silaghi-Dumitrescu, R., *PLoS One* **2018**, *13*, e0200022. <https://doi.org/10.1371/journal.pone.0200022>.
31. Mot, A. C.; Bischin, C.; Muresan, B.; Parvu, M.; Damian, G.; Vlase, L.; Silaghi-Dumitrescu, R., *Nat. Prod. Res.* **2016**, *30*, 1315–1319. <https://doi.org/10.1080/14786419.2015.1054824>.
32. Lehene, M.; Fischer-Fodor, E.; Scurtu, F.; Hădade, N. D.; Gal, E.; Mot, A. C.; Matei, A.; Silaghi-Dumitrescu, R., *Pharmaceuticals*, **2020**, *13*, 107. <https://doi.org/10.3390/PH13060107>.
33. Procházková, D.; Boušová, I.; Wilhelmová, N., *Fitoterapia*. 2011, 513–523. <https://doi.org/10.1016/j.fitote.2011.01.018>.
34. Sánchez-Reus, M. I.; Gómez del Río, M. A.; Iglesias, I.; Elorza, M.; Slowing, K.; Benedí, J., *Neuropharmacology*, **2007**, *52*, 606–616. <https://doi.org/10.1016/j.neuropharm.2006.09.003>.
35. Taciuc, V.; Bischin, C.; Silaghi-Dumitrescu, R., “A Novel Mechanism for Platinum-Based Drugs: Cisplatin and Related Compounds as pro-Oxidants in Blood”, in “Metal Elements in Environment, Medicine and Biology”, Tome IX; Silaghi-Dumitrescu, R., Garban, G. (Eds.), Cluj University Press: Cluj-Napoca, Roumania, 2009, pp. 130–134.
36. Lage, M. Á. P.; García, M. A. M.; Álvarez, J. A. V.; Anders, Y.; Curran, T. P., *Food Res. Int.* **2013**, *53*, 836–846. <https://doi.org/10.1016/J.FOODRES.2012.11.026>.
37. Puscas, C.; Mircea, A.; Raiu, M.; Mic, M.; Attia, A. A. A.; Silaghi-Dumitrescu, R., *Chem. Res. Toxicol.*, **2019**, *32*, 1402–1411. <https://doi.org/10.1021/acs.chemrestox.9b00094>.
38. Moț, A. C.; Coman, C.; Miron, C.; Damian, G.; Sarbu, C.; Silaghi-Dumitrescu, R., *Food Chem.*, **2014**, *143*, 214–222. <https://doi.org/10.1016/j.foodchem.2013.07.128>.
39. Zagrean-Tuza, C.; Igescu, I.; Lupan, A.; Silaghi-Dumitrescu, R., *Inorg. Chim. Acta*, **2024**, *567*, 122053. <https://doi.org/10.1016/j.ica.2024.122053>.
40. Mollan, T. L.; Alayash, A. I., *Antioxid. Redox Signal.*, **2013**, *18*, 2251. <https://doi.org/10.1089/ARS.2013.5195>.
41. Hathazi, D.; Scurtu, F.; Bischin, C.; Mot, A.; Attia, A. A. A.; Kongsted, J.; Silaghi-Dumitrescu, R., *Molecules*, **2018**, *23*, E350. <https://doi.org/10.3390/molecules23020350>.
42. Lanning, M. E.; Yu, W.; Yap, J. L.; Chauhan, J.; Chen, L.; Whiting, E.; Pidugu, L. S.; Atkinson, T.; Bailey, H.; Li, W.; Roth, B. M.; Hynicka, L.; Chesko, K.; Toth, E. A.; Shapiro, P.; MacKerell, A. D.; Wilder, P. T.; Fletcher, S., *Eur. J. Med. Chem.*, **2016**, *113*, 273–292. <https://doi.org/10.1016/J.EJMECH.2016.02.006>.
43. Chandrasekhar, S.; Prasad, K. N. N.; Balasaraswathy, S.; Raghu, M. S.; Prashanth, M. K.; Alharethy, F.; Jeon, B.-H., *J. Biomol. Struct. Dyn.*, **2025**, 1–12. <https://doi.org/10.1080/07391102.2025.2490792>.
44. Zelenović, N.; Ristić, P.; Polović, N.; Todorović, T.; Kojadinović, M.; Popović, M., *Molecules*, **2024**, *29*, 4474. <https://doi.org/10.3390/molecules29184474>.
45. Chaves, O. A.; Cesarin-Sobrinho, D.; Serpa, C.; da Silva, M. B.; de Lima, M. E. F.; Netto-Ferreira, J. C., *Int. J. Biol. Macromol.*, **2024**, *283*, 137981. <https://doi.org/10.1016/j.ijbiomac.2024.137981>.
46. Petitpas, I.; Grüne, T.; Bhattacharya, A. A.; Curry, S., *J. Mol. Biol.*, **2001**, *314*, 955–960. <https://doi.org/10.1006/JMBI.2000.5208>.
47. Safo, M. K.; Abraham, D. J., *Biochemistry*, **2005**, *44*, 8347–8359. <https://doi.org/10.1021/bi050412q>.
48. Zăgrean-Tuza, C.; Matei, A.; Silaghi-Dumitrescu, R., *J. Inorg. Biochem.*, **2024**, 112613. <https://doi.org/10.1016/J.JINORGBIO.2024.112613>.
49. Drew, H. R.; Wing, R. M.; Takano, T.; Broka, C.; Tanaka, S.; Itakura, K.; Dickerson, R. E., *Proc. Natl. Acad. Sci.*, **1981**, *78*, 2179–2183. <https://doi.org/10.1073/PNAS.78.4.2179>.
50. Hathazi, D.; Mot, A. C.; Vaida, A.; Scurtu, F.; Lupan, I.; Fischer-Fodor, E.; Damian, G.; Kurtz Jr., D. M.; Silaghi-Dumitrescu, R., *Biomacromolecules*, **2014**, *15*, 1920–1927. <https://doi.org/10.1021/bm5004256>.
51. Frisch, M. J.; Trucks, G. W.; Schlegel, H. B.; Scuseria, G. E.; Robb, M. A.; Cheeseman, J. R.; Scalmani, G.; Barone, V.; Petersson, G. A.; Nakatsuji, H.; Li, X.; Caricato, M.; Marenich, A. V.; Bloino, J.; Janesko, B. G.; Gomperts, R.; Mennucci, B.; Hratchian, H. P.; Ortiz, J. V.; Izmaylov, A. F.; Sonnenberg, J. L.; Williams-Young, D.; Ding, F.; Lipparini, F.; Egidi, F.; Goings, J.; Peng, B.; Petrone, A.; Henderson, T.; Ranasinghe, D.; Zakrzewski, V. G.; Gao, J.; Rega, N.; Zheng, G.; Liang, W.; Hada, M.; Ehara, M.; Toyota, K.; Fukuda, R.; Hasegawa, J.; Ishida, M.; Nakajima, T.; Honda, Y.; Kitao, O.; Nakai, H.; Vreven, T.; Throssell, K.; Montgomery, J. A., Jr.; Peralta, J. E.; Ogliaro, F.; Bearpark, M. J.; Heyd, J. J.; Brothers, E. N.; Kudin, K. N.; Staroverov, V. N.; Keith, T. A.; Kobayashi, R.; Normand, J.; Raghavachari, K.; Rendell, A. P.; Burant, J. C.; Iyengar, S. S.; Tomasi, J.; Cossi, M.; Millam, J. M.; Klene, M.; Adamo, C.; Cammi, R.; Ochterski, J. W.; Martin, R. L.; Morokuma, K.; Farkas, O.; Foresman, J. B.; Fox, D. J. Gaussian 16, Revision C.01. Gaussian, Inc.: Wallingford, CT 2016.
52. Stoean, B.; Lehene, M.; Zagrean-Tuza, C.; Silaghi-Dumitrescu, R.; Cristea, C.; Găina, L., *Spectrochim. Acta Part A Mol. Biomol. Spectrosc.*, **2024**, *320*, 124602. <https://doi.org/10.1016/J.SAA.2024.124602>.
53. Lee, C.; Yang, W.; Parr, R. G., *Phys. Rev. B*, **1988**, *37*, 785–789. <https://doi.org/10.1103/PhysRevB.37.785>.
54. Schäfer, A.; Horn, H.; Ahlrichs, R., *J. Chem. Phys.*, **1992**, *97*, 2571–2577. <https://doi.org/10.1063/1.463096>.
55. Forli, S.; Huey, R.; Pique, M. E.; Sanner, M.; Goodsell, D. S.; Arthur, J. 00006565-201002000-00017. **2016**, *11*, 905–919. <https://doi.org/10.1038/nprot.2016.051>. Computational.

